
CONDENSED-MATTER SPECTROSCOPY

Exciton Absorption Spectra of Cs_2CdI_4 and Rb_2CdI_4 Ferroelastic Solid Solutions

V. K. Miloslavskii^a, O. N. Yunakova^a, and E. N. Kovalenko^b

^a Kharkov National University, Kharkov, 61077 Ukraine

^b Kharkov National University of Radioelectronics, Kharkov, 61166 Ukraine

e-mail: Vladimir.K.Miloslavsky@univer.kharkov.ua; Olga.N.Yunakova@univer.kharkov.ua

Received June 16, 2010

Abstract—The exciton absorption spectra of thin films of $(\text{Cs}_{1-x}\text{Rb}_x)_2\text{CdI}_4$ solid solutions have been investigated and the refractive index $n(\lambda)$ in their transparency window in the concentration range of $0 \leq x \leq 1$ has been measured. The exciton-band parameters and optical permittivity $\varepsilon_{\infty}(x)$ have been found to linearly depend on the concentration. It is established that excitons are incorporated into the CdI_2 sublattice of the solid solutions and belong to intermediate-coupling ones. The characteristics of excitons in ferroelastics are compared with the corresponding parameters for CdI_2 , RbI , and CsI , which are used as components to synthesize ternary compounds.

DOI: 10.1134/S0030400X10120131

$M_2\text{CdI}_4$ compounds ($M = \text{Cs}, \text{Rb}$) belong to incommensurate ferroelastics. In the ordered commensurate phase both compounds have an orthorhombic lattice of the $\beta\text{-K}_2\text{SO}_4$ type with similar parameters: $a = 1.074$ and 1.06 nm, $b = 0.846$ and 0.84 nm, and $c = 1.485$ and 1.49 nm in Cs_2CdI_4 and Rb_2CdI_4 , respectively (sp. gr. P_{nma} , $z = 4$) [1–3]. The isostructurality of $M_2\text{CdI}_4$ compounds and close values of their lattice parameters facilitate the formation of $(\text{Cs}_{1-x}\text{Rb}_x)_2\text{CdI}_4$ solid solution in the entire concentration range.

The absorption spectra of $M_2\text{CdI}_4$ ($M = \text{Cs}, \text{Rb}$) were previously investigated in [3]. It was established that both compounds belong to direct-gap insulators and that low-frequency exciton excitations are localized in the structural elements of the their lattice, CdI_4^{2-} . In this localization, the top of the valence band in $M_2\text{CdI}_4$ is formed by I 5p states and Cd 4d states, while the lower conduction band is formed by the Cd 5s states [3].

In this paper, we report the results of studying the absorption spectra and dispersion of the refractive indices of $(\text{Cs}_{1-x}\text{Rb}_x)_2\text{CdI}_4$ solid solutions in the concentration range of $0 \leq x \leq 1$.

EXPERIMENTAL

$(\text{Cs}_{1-x}\text{Rb}_x)_2\text{CdI}_4$ solid solutions were synthesized by vacuum alloying of pure CsI , RbI , and CdI_2 powders, taken in a specified molar ratio. Thin films were prepared by thermal deposition of the alloy in vacuum onto quartz substrates heated to 100°C , according to

the technique [3]; the deposited films were annealed for 1 h at the same temperature.

The quality and phase composition of the films were determined by measuring absorption spectra at $T = 90$ K. The phase composition can be optically monitored because the spectral positions of the long-wavelength exciton bands in $(\text{Cs}_{1-x}\text{Rb}_x)_2\text{CdI}_4$ (4.63–4.65 eV), CdI_2 (4.03 eV [4]), CsI (5.8 eV), and RbI (5.74 eV) significantly differ.

The absorption spectra were measured on (100–150)-nm thick films, using an SF-46 spectrophotometer, in a spectral range of 2–6 eV at temperatures $T = 90$ K ($0 \leq x \leq 1$) and 290 K ($x = 0$ or 1). The measurements were performed at 11 x values with a step $\Delta x = 0.1$.

The parameters of the long-wavelength exciton bands (position E_m ; half-width Γ ; and imaginary part of permittivity in the band peak, ε_{2m}) were determined using the technique [5] by approximating the experimental dependence of optical density with a mixed symmetric profile (a linear combination of Lorentzian and Gaussian profiles). The approximation was used to obtain the best agreement between the calculated profile and the measured optical density spectra $D = -\ln t$ at the long-wavelength slope of the bands.

The refractive index $n(\lambda)$ of the $(\text{Cs}_{1-x}\text{Rb}_x)_2\text{CdI}_4$ solid solutions was determined in a spectral range of 300–1000 nm by the interference method from the transmission spectra of the films. To this end, we used rather thick films ($t \sim 800$ –900 nm), whose transmission spectra $T(\lambda)$ contained several interference extrema in the transparency range. The dispersion of constants is generally low in this range; therefore, the

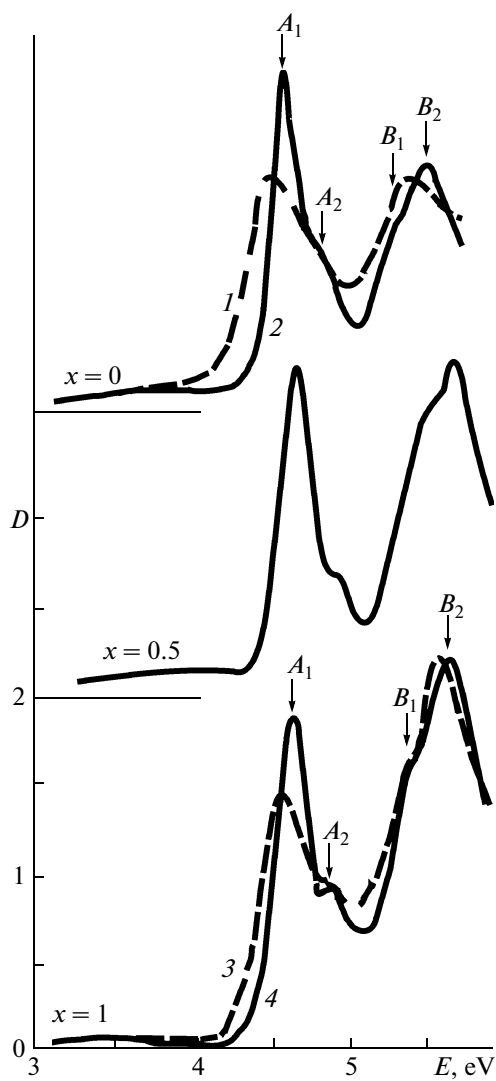


Fig. 1. Absorption spectra of thin $(\text{Cs}_{1-x}\text{Rb}_x)_2\text{CdI}_4$ films, recorded at $T = (1, 3) 290$ and $(2, 4) 90$ K.

extreme transmission values are obtained under the condition $4nt = m\lambda$, where m are even and odd integers for maxima and minima, respectively. The film thickness was measured by an MII-4 Linnik interferometer. The unknown interference order m was found from the spectral position of neighboring maxima or minima. The refractive index was calculated from the aforementioned formula.

ABSORPTION SPECTRA OF THIN $(\text{Cs}_{1-x}\text{Rb}_x)_2\text{CdI}_4$ FILMS

The absorption spectra of thin $(\text{Cs}_{1-x}\text{Rb}_x)_2\text{CdI}_4$ films ($0 \leq x \leq 1$) have a similar structure and position of the main bands (Fig. 1). The spectra at $T = 90$ K exhibit a strong A_1 band, a weaker A_2 band, and high-frequency B_1 and B_2 bands. With an increase in tem-

perature the A and B bands shift to longer wavelengths, broaden, and become weaker due to the exciton–phonon interaction (EPI), which indicates their relationship with exciton excitations.

The spacings between the A and B bands, $\Delta E_{AB} = \bar{E}_{B_1, B_2} - \bar{E}_{A_1, A_2} = 0.705$ and 0.74 eV for Cs_2CdI_4 and Rb_2CdI_4 , respectively; these values are intermediate between the spin–orbit (SO) splittings of the valence band in CdI_2 ($\Delta_{\text{CO}} = 0.54$ eV [6]) and in CsI and RbI ($\Delta_{\text{CO}} = 1.06$ and 1.2 eV, respectively [7]) and apparently correspond to the SO splitting in $M_2\text{CdI}_4$ ($M = \text{Cs}, \text{Rb}$). For binary compounds, the SO splitting of the top of the valence band is determined by the relation

$$\Delta_{\text{CO}} = C(\xi^{(1)}\Delta_{\text{CO}}^{(1)} + \xi^{(2)}\Delta_{\text{CO}}^{(2)}), \quad (1)$$

where $\Delta_{\text{CO}}^{(1,2)}$ is the SO splitting of the atomic spectrum and $\xi^{(1,2)}$ characterizes the contribution of each type of atoms into the SO splitting of the compound ($\xi^{(1)} + \xi^{(2)} = 1$) [7]. Having generalized formula (1) to ternary compounds, assuming that $\Delta_{\text{CO}}^{(1)} = \Delta_{\text{CO}}(\text{CdI}_2) = 0.54$ eV, and $\Delta_{\text{CO}}^{(2)} = \Delta_{\text{CO}}(\text{CsI}) = 1.06$ eV [7], and supposing that, for Cs_2CdI_4 $\Delta_{\text{CO}} = 0.705$ eV (while for Rb_2CdI_4 $\Delta_{\text{CO}} = 0.74$ eV and $\Delta_{\text{CO}}^{(2)} = \Delta_{\text{CO}}(\text{RbI}) = 1.2$ eV [7]), we found from (1) that $\xi^{(1)} = 0.68$ and 0.69 and $\xi^{(2)} = 0.32$ and 0.31 for Cs_2CdI_4 and Rb_2CdI_4 , respectively. Hence, the main contribution to the SO splitting in $M_2\text{CdI}_4$ is from the CdI_2 sublattice, which additionally confirms localization of exciton excitations in CdI_4^{2-} tetrahedra of the compounds.

With a decrease in temperature, the A and B exciton bands in $(\text{Cs}_{1-x}\text{Rb}_x)_2\text{CdI}_4$ are split into A_1 , A_2 , B_1 , and B_2 bands. The splitting of the A bands ($\Delta E_A = E_{A_2} - E_{A_1} = 0.24$ ($x = 0$) and 0.29 eV ($x = 1$)) and the B bands ($\Delta E_B = E_{B_2} - E_{B_1} = 0.25$ ($x = 0$) and 0.28 eV ($x = 1$)) are similar, which indicates the general nature of splitting for both of these bands.

To reveal the nature of splitting of A and B exciton bands, we will consider the structure of the crystal lattice of Cs_2CdI_4 and Rb_2CdI_4 compounds in more detail. As was noted above, both these compounds are layered crystals of the $\beta\text{-K}_2\text{SO}_4$ type, with layers oriented perpendicularly to the c axis. CdI_4 tetrahedra are located in the (ab) plane. The bond lengths $d_{\text{Cd}-\text{I}}$ in Cs_2CdI_4 vary from 0.274 to 0.313 nm; i.e., the tetrahedra are somewhat distorted and the $d_{\text{Cd}-\text{I}}$ distance is much smaller than the sum of the Pauling ionic radii ($d_{\text{Cd}-\text{I}} = 0.313$ nm), which indicates a contribution of covalent bonding. Cs^+ ions with $d_{\text{Cs}-\text{I}} = 0.385$ – 0.428 nm, a value similar to the sum of ionic radii ($d_{\text{Cs}-\text{I}} = 0.385$ nm), are located between tetrahedra both inside and between the layers. The structure of

Rb_2CdI_4 crystals is similar to the above-described Cs_2CdI_4 structure.

The translational exciton transfer between equivalent tetrahedra is most efficient along the short \mathbf{b} axis. There is another tetrahedron between equivalent tetrahedra, which is somewhat shifted with respect to the \mathbf{b} axis (with $d_{\text{Cd}-\text{Cd}} = 0.546$ nm for Cs_2CdI_4 and 0.54 nm for Rb_2CdI_4 , according to our estimates). The exciton transfer between neighboring nonequivalent tetrahedra should lead to Davydov splitting of exciton bands [8]. Apparently, the splitting of the A and B bands in the Cs_2CdI_4 and Rb_2CdI_4 spectra is related to the Davydov splitting of exciton bands [9].

With an increase in the concentration x the intensity of B bands in the absorption spectra of $(\text{Cs}_{1-x}\text{Rb}_x)_2\text{CdI}_4$ increases (Fig. 1); this increase is apparently caused by the superposition of the exciton absorption in the $\text{Cs}_{1-x}\text{Rb}_x\text{I}$ sublattice with the B_2 band. In the CsI and RbI spectra the long-wavelength exciton band is located at 5.8 eV (90 K) and 5.74 eV, respectively. With an increase in x the exciton band of the $\text{Cs}_{1-x}\text{Rb}_x\text{I}$ sublattice is nonlinearly red-shifted [10]. The B_2 band of $(\text{Cs}_{1-x}\text{Rb}_x)_2\text{CdI}_4$, on the contrary, is blue-shifted with an increase in x : from 5.6 ($x = 0$) to 5.65 ($x = 1$) eV. Note also that the intensity of B bands is also overestimated because of their superposition with the continuous spectrum of interband absorption, which is adjacent to A bands.

The interaction of B excitons with the continuous spectrum leads to their self-trapping and additional broadening of the B bands. The half-width of the B_1 bands ($\Gamma(1) = 0.32$ eV) and B_2 bands ($\Gamma(1) = 0.34$ eV) at $x = 1$ greatly exceeds the half-width of the A_1 bands ($\Gamma(1) = 0.22$ eV) and A_2 bands ($\Gamma(1) = 0.25$ eV). The parameters of the high-frequency B_1 and B_2 exciton bands are difficult to determine precisely because it is a serious problem to cut off the continuous spectrum. Therefore, we investigated the concentration dependences of the spectral position $E_m(x)$ and half-width $\Gamma(x)$ for only low-frequency A_1 and A_2 exciton bands (Fig. 2).

The concentration dependences $E_m(x)$ and $\Gamma(x)$ are linear and have the form

$$E_m(x) = E_m(0) + ax \quad (2a)$$

$$\Gamma(x) = \Gamma(0) + Ax, \quad (2b)$$

where $E_m(0) = 4.65$ and 4.89 eV, $a = dE_m/dx = -1.2 \times 10^{-3}$, and 3×10^{-3} eV, $\Gamma(0) = 0.18$ and 0.25 eV, and $A = d\Gamma/dx = 4.5 \times 10^{-3}$ and 0 eV for the A_1 and A_2 bands, respectively. In the case of binary solid solutions the dependence $E_m(x)$ generally exhibits a low-frequency deflection at $x \approx 0.5$, and the function $\Gamma(x)$ reaches a maximum at $x \approx 0.5$. These deviations from linearity are due to the small-scale composition fluctuations, caused by solid solution disorder, and large-scale fluctuations, related to the sample preparation

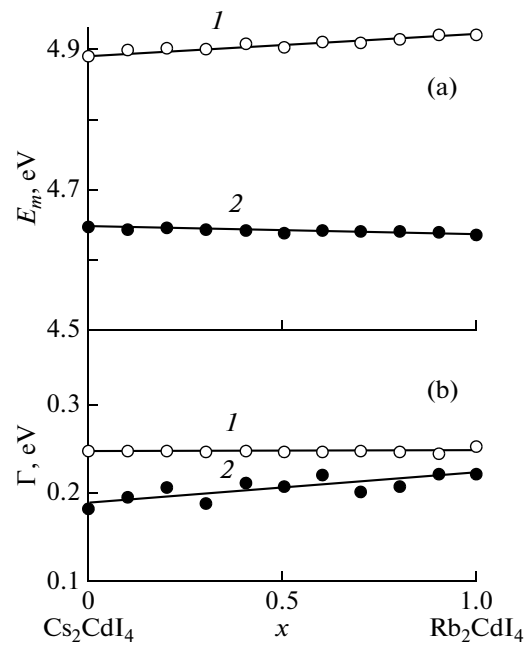


Fig. 2. Concentration dependences of (a) spectral position $E_m(x)$ and (b) half-width $\Gamma(x)$ of long-wavelength exciton bands (2) A_1 and (1) A_2 in thin $(\text{Cs}_{1-x}\text{Rb}_x)_2\text{CdI}_4$ films.

technique. The linear run of the concentration dependences of the spectral position of exciton bands, $E_m(x)$, and the half-width $\Gamma(x)$ for $(\text{Cs}_{1-x}\text{Rb}_x)_2\text{CdI}_4$ confirms that the exciton excitations are localized in lattice structural CdI_4^{2-} elements.

To reveal the character of exciton states in $(\text{Cs}_{1-x}\text{Rb}_x)_2\text{CdI}_4$, one must estimate the exciton radius a_{ex} . We will previously calculate the optical permittivity $\varepsilon_\infty(x)$, which must be done to determine a_{ex} .

DISPERSION OF REFRACTIVE INDEX $n(\lambda)$ IN THIN $(\text{Cs}_{1-x}\text{Rb}_x)_2\text{CdI}_4$ FILMS

The spectral dependences $n(\lambda)$ for different x (Fig. 3), obtained by the above-described technique, are described well in terms of the single-oscillator model as follows [11]:

$$\varepsilon_1 = n^2 = 1 + \frac{E_d E_0}{E^2 - E_0^2}, \quad (3)$$

where $E = \hbar\omega$, E_0 , and E_d are the parameters of the single-oscillator model. E_0 determines the spectral position of the effective oscillator related to interband optical transitions. The E_0 value exceeds E_g and is close to the maximum of the electronic absorption band [11]. E_d is the dispersion energy, which characterizes the interband-transition strength.

As follows from (3), the dependence of $(n^2 - 1)^{-1}$ on E^2 should be linear, which is confirmed by its plot constructed using the found $n(\lambda)$ values in the range

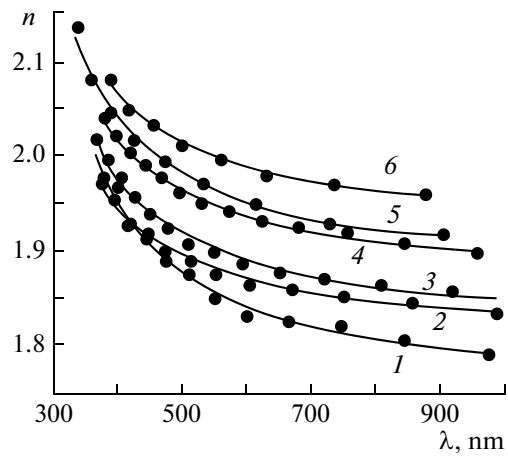


Fig. 3. Spectral dependences of refractive index $n(\lambda)$ of thin $(\text{Cs}_{1-x}\text{Rb}_x)_2\text{CdI}_4$ films with $x = (1) 0, (2) 0.2, (3) 0.4, (4) 0.6, (5) 0.8$, and (6): (circles) experimental and (solid lines) theoretical data (3).

$\lambda = 350\text{--}1000$ nm and in the entire range of x . The concentration dependences $E_0(x)$ and $E_d(x)$ (Fig. 4) were found to be linear:

$$E_0(x) = E_0(0) - b_0 x, \quad (4a)$$

$$E_d(x) = E_d(0) - b_d x, \quad (4b)$$

where $E_0(0) = 7.5 \pm 0.3$ eV, $b_0 = dE_0/dx = 1.1 \pm 0.5$ eV, $E_d(0) = 19.3 \pm 0.8$ eV, and $b_d = dE_d/dx = 5.9 \pm 1.4$ eV. The dependences $n(\lambda)$ calculated from (3) with the found E_0 and E_d values are in good agreement with the experimental results (Fig. 3). As was noted above, $E_0 > E_g$, which is in agreement with the experimental data [3]. It was shown in [11] that E_d is proportional to the density ρ of the material; i.e., E_d characterizes the film porosity. Apparently, large deviations of the experimental values $E_d(x)$ from the linear dependence (4b) are due to the change in the film porosity from sample to sample.

EXCITON STATES IN Cs_2CdI_4 AND Rb_2CdI_4

The results obtained make it possible to study in more detail the exciton states, which determine the spectral position of the long-wavelength bands in Cs_2CdI_4 and Rb_2CdI_4 and their solid solutions and perform a comparison with the exciton characteristics of CdI_2 and MI .

As follows from (3), the extrapolation of $\hbar\omega = E$ to zero frequency yields the optical permittivity $\varepsilon_\infty = 1 + E_d/E_0$, an important constant that is used in the analysis of excitons in crystals with an intermediate electron-hole coupling [12]. The data in Fig. 4 suggest a

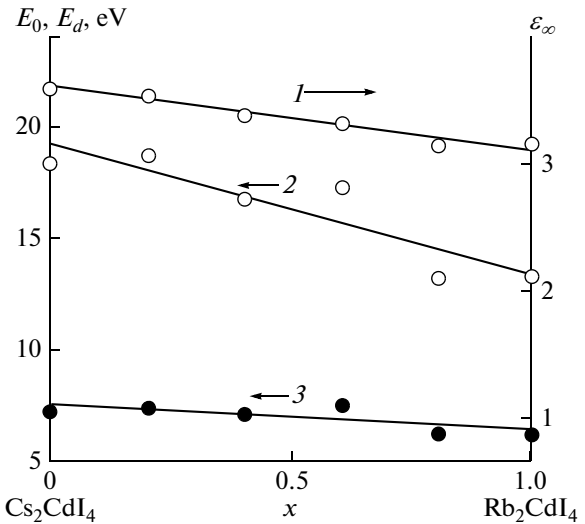


Fig. 4. Concentration dependences of parameters of single-oscillator model, (3) $E_0(x)$ and (2) $E_d(x)$, and (1) the optical permittivity $\varepsilon_\infty(x)$.

linear falloff of $\varepsilon_\infty(x)$ with an increase in the Rb concentration:

$$\varepsilon_\infty(x) = \varepsilon_\infty(0) - (d\varepsilon_\infty/dx)x. \quad (5)$$

A treatment of this dependence by the least-squares method yielded $\varepsilon_\infty(0) = 3.58 \pm 0.04$ and $d\varepsilon_\infty/dx = 0.49 \pm 0.06$. It is interesting to compare the found $\varepsilon_\infty(0)$ and $\varepsilon_\infty(1)$ values with the corresponding values for CsI and RbI (3.05 and 2.72, respectively) and for CdI_2 (4.05), components in synthesis of ternary compounds. The value of 4.05 was found by measuring $n(\lambda)$ in thin CdI_2 films and treating the measurement results according to formula (3). For comparison we will apply the interpolation formula

$$\varepsilon_\infty(\text{M}_2\text{CdI}_4) = 0.67\varepsilon_\infty(\text{MI}) + 0.33\varepsilon_\infty(\text{CdI}_2). \quad (6)$$

A calculation according to (6) yields $\varepsilon_\infty = 3.38$ for Cs_2CdI_4 and 3.17 for Rb_2CdI_4 , values that agree with the results of direct measurements (3.57 and 3.14) for these compounds.

As was mentioned above, we believe the difference $E_{A2} - E_{A1}$ to be due to the Davydov splitting of exciton bands, caused by the interaction of excitons in non-equivalent tetrahedra in the M_2CdI_4 crystal lattice. This fact was established when studying the spectra of $\text{Cs}_2(\text{Cd}_{1-x}\text{Zn}_x)\text{I}_4$ solid solutions [9]; it hinders estimation of the exciton binding energy R_{ex} in ternary compounds. The R_{ex} value was determined in the following way. The band gap E_g in M_2CdI_4 was found from the inflection point of the continuous-spectrum edge after separation of the A_0 and A_1 bands from the interband absorption edge. Hence, $E_g = 4.96$ and 4.89 eV for Cs_2CdI_4 and Rb_2CdI_4 , respectively [3]. The R_{ex} values were determined from the difference $R_{\text{ex}} = E_g - E_{A1}$;

they turned out to be 0.31 and 0.28 eV. Taking into account that the R_{ex} values are close at $x \neq 0$ and 1 and that the dependence $E_{A1}(x)$ is linear, we did not determine E_{A1} at other x values.

With the R_{ex} and ε_{∞} values known, one can find the exciton radius, because within the Wannier–Mott model the 1s-exciton radius obeys the relation

$$a_{\text{ex}} = a_B \frac{R}{R_{\text{ex}} \varepsilon_{\text{ef}}}, \quad (7)$$

where $a_B = 0.529 \times 10^{-8}$ cm is the Bohr radius, $R = 13.6$ eV is the Rydberg constant, ε_{ef} is the permittivity determining the electron–hole Coulomb coupling ($\varepsilon_{\infty} < \varepsilon_{\text{ef}} < \varepsilon_0$), and ε_0 is the static permittivity. For resonant frequencies, which determine the exciton excitation in the compounds studied, it is natural to assume that $\varepsilon_{\text{ef}} = \varepsilon_{\infty}$ because the resonant frequencies significantly exceed the eigenfrequencies. In other words, the exciton excitation is not accompanied by atomic displacements. Hence, with the found R_{ex} and ε_{∞} values, formula (7) yields $a_{\text{ex}} = 6.5$ Å for Cs_2CdI_4 and 8.2 Å for Rb_2CdI_4 .

Let us compare the found characteristics of the exciton states in these compounds with the corresponding characteristics for CdI_2 , RbI , and CsI —components for synthesizing ferroelastics.

CdI_2 is known to be an indirect-gap insulator. However, we found that the introduction of a small amount ($x \cong 0.01$) of Zn impurity into CdI_2 leads to the following effects: absorption vanishes in the indirect-transition range (3.5–4 eV); the X_1 exciton band at 3.93 eV due to direct transitions is enhanced; and a weaker band is formed at 4.12 eV [13]. Based on these data, we found $R_{\text{ex}} = 0.2$ eV and $E_g = 4.17$ eV. This E_g value is close to the theoretical estimate $E_g = 4.03$ eV [6] for direct transitions in CdI_2 . To evaluate a_{ex} in CdI_2 , we used $\varepsilon_{\infty} = 4.05$ in (7); hence, $a_{\text{ex}} = 8.9$ Å.

The exciton absorption spectra of RbI and CsI were investigated in the early studies [14–16] devoted to the transmission of thin iodide films deposited on transparent crystalline substrates. The long-wavelength part of the absorption spectrum in RbI is fairly simple and consists of a narrow strong band at 5.74 eV (10 K), which corresponds to the excitation of exciton with a principal quantum number $n = 1$, and a much weaker band at 6.12 eV that corresponds to $n = 2$. Based on these data, we found (within the Wannier–Mott model) E_g , R_{ex} , and $a_{\text{ex}} = 4.55$ Å [15]. The absorption spectrum of CsI is more complex, because it contains several long-wavelength exciton peaks with $n = 1$; in this context, the electronic bands and exciton spectrum of this compound were investigated in several experimental [14, 16] and theoretical [17, 18] studies. In [14], the positions of the longest wavelength peak at 5.81 eV ($n = 1$) and a weaker peak at 6.23 eV ($n = 2$) were used to find E_g and R_{ex} , and we calculated a_{ex} to

Characteristics of exciton states in the compounds

Compound	E_g , eV	R_{ex} , eV	ε_{∞}	a_{ex} , Å
Rb_2CdI_4	4.89	0.28	3.14	8.20
Cs_2CdI_4	4.96	0.31	3.57	6.50
CdI_2	4.17	0.20	4.05	8.9
RbI	6.26	0.58	2.72	4.550
CsI	6.37	0.56	3.05	4.750

be 4.75 Å from the ε_{∞} value. The assignment of the weak peak at 6.23 eV to the 2s exciton was also confirmed by the calculation of the structure of electronic bands in CsI in [18], where it was shown that excitons in CsI are genetically related to the p -like valence band and s - and d -like conduction bands at the point Γ of the Brillouin zone.

The characteristics of excitons in Rb_2CdI_4 , Cs_2CdI_4 , CdI_2 , RbI , and CsI are listed in table. The data on E_g , R_{ex} , and a_{ex} suggest the following. All these characteristics of Rb_2CdI_4 and Cs_2CdI_4 have intermediate values between the corresponding values for CdI_2 and RbI , CsI ; however, the E_g and R_{ex} values in ferroelastics are closer to these in CdI_2 rather than in MI . This is evidenced by the following. The difference $\Delta E_g = E_g(\text{Rb}_2\text{CdI}_4) - E_g(\text{CdI}_2) = 0.72$ eV, whereas $E_g(\text{RbI}) - E_g(\text{Rb}_2\text{CdI}_4) = 1.44$ eV; the similar differences for the Cs-containing compounds are 0.79 and 1.41 eV, despite the fact that there are two MI molecules per CdI_2 molecule in ferroelastics. From the point of view of the LCAO method, these results indirectly indicate a smaller contribution of the wave functions of Rb and Cs (in comparison with these of Cd and I) to the formation of the conduction- and valence-band edges, adjacent to the band gap in M_2CdI_4 . This conclusion is confirmed by the differences for R_{ex} : $\Delta R_{\text{ex}} = R_{\text{ex}}(\text{Rb}_2\text{CdI}_4) - R_{\text{ex}}(\text{CdI}_2) = 0.08$ eV and $R_{\text{ex}}(\text{RbI}) - R_{\text{ex}}(\text{Rb}_2\text{CdI}_4) = 0.3$ eV, whereas for the Cs-containing compounds the corresponding values are 0.11 and 0.25 eV, respectively. The data on ΔR_{ex} and, especially, Δa_{ex} indicate a stronger localization of excitons in CdI_2^{2+} tetrahedra of the Rb_2CdI_4 ferroelastic in comparison with Cs_2CdI_4 .

We should emphasize that these conclusions are only qualitative, because the data compared are for compounds with different crystal lattices: cubic (MI), hexagonal (CdI_2), and orthorhombic (M_2CdI_4). Their anisotropy indicates that the principal components of the tensor ε should differ; however, we disregarded it in our analysis. As the experiment showed, the layered character of CdI_2 and M_2CdI_4 facilitates crystallites in thin films to be oriented with their c axis directed perpendicularly to the substrate plane; i.e., the found ε_{∞} values are ε_{\perp} for CdI_2 and $\overline{\varepsilon}_{\perp}$ for M_2CdI_4 ($\overline{\varepsilon}_{\perp} = 0.5(\varepsilon_a + \varepsilon_b)$). More exact data on the absorption spectra of

$M_2\text{CdI}_4$ could be gained by depositing films on the corresponding transparent crystalline substrates; however, the latter are difficult to obtain. Nevertheless, this analysis is useful for the further study of the electronic and exciton bands of $M_2\text{CdI}_4$.

CONCLUSIONS

We investigated the exciton absorption spectra of thin films of Rb_2CdI_4 and Cs_2CdI_4 ferroelastics and their solid solutions $(\text{Cs}_{1-x}\text{Rb}_x)_2\text{CdI}_4$, as well as the refractive index dispersion in the range of their transparency. The data obtained revealed a linear concentration behavior of the spectral position of the long-wavelength exciton A bands and their half-width, the spin-orbit interaction energy, and the optical permittivity. All of these data were used to compare the characteristics of excitons in $M_2\text{CdI}_4$ with the corresponding parameters for CdI_2 , RbI , and CsI compounds, which are used to synthesize ferroelastic crystals. The results of comprehensive analysis indicate that the exciton states are better localized in the CdI_2 sublattice of Rb_2CdI_4 in comparison with Cs_2CdI_4 and that the excitons in ferroelastics belong to the excitons involved in intermediate Coulomb coupling.

REFERENCES

- K. S. Aleksandrov, S. V. Melnikova, I. N. Flerov, A. D. Vasilev, A. I. Kruglik, and I. I. Kokov, *Phys. Status Solidi A* **105**, 441 (1988).
- V. Touchard, V. Louer, J. P. Auffredic, and D. Louer, *Rev. Chim. Miner.* **24**, 414 (1987).
- O. N. Yunakova, V. K. Miloslavsky, and E. N. Kovalenko, *Fiz. Nizk. Temp. (Kiev)* **29** (8), 922 (2003).
- M. K. Tubbs, *J. Phys. Chem. Solids* **29** (7), 1191 (1968).
- O. N. Yunakova, V. K. Miloslavsky, and E. N. Kovalenko, *Opt. Spektrosk.* **104** (4), 631 (2008) [*Opt. Spectrosc.* **104** (4), 552 (2008)].
- I. Pollini, J. Tomas, R. Coehoorn, and C. Haas, *Phys. Rev. B* **33**, 5747 (1986).
- M. Cardona, *Modulation Spectroscopy* (Academic, New York, 1969; Mir, Moscow, 1972), p. 416.
- A. S. Davydov, *Theory of Molecular Excitons* (Nauka, Moscow, 1968) [in Russian].
- V. K. Miloslavsky, O. N. Yunakova, and E. N. Kovalenko, *Opt. Spektrosk.* **108** (4), 653 (2010).
- T. Hirai and S. Hashimoto, *Proc. of EXCON'96, the 2nd International Conference on Excitonic Processes in Condensed Matter* (Dresden Univ. Press, Dresden, 1966), p. 167.
- S. H. Wemple, *Phys. Rev. B* **7** (8), 3767 (1973).
- F. Bassani and G. P. Parravicini, *Electronic States and Optical Transitions in Solids* (Pergamon, Oxford, 1975; Nauka, Moscow, 1982), p. 391.
- O. N. Yunakova, V. K. Miloslavsky, and E. N. Kovalenko, *Fiz. Nizk. Temp. (Kiev)* **28** (4), 406 (2002).
- F. Fisher and R. Hilsch, *Nacht. Acad. Wiss. Göttingen II Math.-Phys. K1* (8) (1959).
- J. Ramamurti and K. Teegarden, *Phys. Rev.* **145** (2), 698 (1966).
- K. Teegarden and G. Baldini, *Phys. Rev.* **136** (6A), 1721 (1964).
- J. C. Phillips, *Phys. Rev.* **155** (3), 896 (1967).
- J. Onodera, *J. Phys. Soc. Jpn.* **25** (2), 469 (1868).

Translated by Yu. Sin'kov